

Filaments in the TGBA phase

Lubor Lejček*, Vladimíra Novotná, and Milada Glogarová

Institute of Physics, the Czech Academy of Sciences, Na Slovance 2, 182 21 Prague 8, Czech Republic

Abstract

A model of filaments of the TGBA phase arising from the homeotropic smectic A phase and nucleating on the sample surface is proposed. The model is based on the concept of finite blocks of parallel smectic layers forming a helical structure. The blocks are surrounded by dislocation loops. The model describes the filament structure near the sample surface and explains the observed inclination of the filament axis with respect to the easy direction of the molecular anchoring on the surface. The model is based on the observations of filament textures of the TGBA phase in a new chiral liquid crystalline compound, but can be applied for forming of TGBA filaments in any compound. The compression modulus of the compound has been estimated using such parameters as anchoring energy, estimated from the field necessary to transform the structure into the homeotropic smectic A, and the observed filament width.

1. Introduction

Twist grain boundary (TGB) phases in liquid crystalline compounds with chiral molecules are the frustrated phases existing due to the competing intermolecular interactions and strong molecular chirality, which lead both to the assembly of molecules in layers and the formation of spiral structures. The structures of these phases are inevitably accompanied with defects having the significant consequences on their nucleation, textures and then on their properties.

The TGBA phase, which is the object of this study, is composed of blocks (slabs) of the orthogonal smectic A. Due to chirality they rotate about an axis lying in the smectic layers, the pitch of rotation being typically in the range of the visible light wave length. The blocks (slabs) are separated by systems of screw dislocations forming *twist boundary* analogously as in solids where crystal grains are separated by screw dislocations [1]. The existence of TGB phases was first predicted by de Gennes [2], theoretically described by Renn et al. [3] and afterwards discovered by Goodby [4]. So far there is a lot of papers reporting the existence of TGB phases in various compounds and describing their properties. Typically the TGB phases occur below the Blue phase or the cholesteric phase, but may appear directly below the isotropic phase. There is also a case when TGBA phase appears as a reentrant phase below the smectic A phase [5].

The textures of TGB phases exhibit various features depending on the sample thickness, surface [6] and geometries [7]. Besides, paramorphic textures from the neighboring phase survive in the TGB phase and in the opposite, the features of TGB textures persist in the non-frustrated

*Corresponding author: lejcekl@fzu.cz

phase. The reason is the inevitable presence of defects in the TGB phases, which have to be melted in the other next phases. Generally, the textures of the TGB phases are diverse and complicated. In free standing films, as well as in samples with homeotropic anchoring, the filament or fingerprint textures typically occur [5-12]. Nevertheless, under the homeotropic anchoring also features similar to the fan-shaped textures known from classical smectic phases may be observed in the TGB phases [6,8]. Under the planar anchoring a blurred fan-shaped texture [6], oily streaks structure or irregular grains can appear. In the grain texture the color corresponds to the pitch length of the TGB block rotating, the rotation axis being perpendicular to the sample plane [5-8].

Here we report a model of filaments nucleating from the homeotropic smectic A phase. The model is based on the experiment performed on PHB(S) compound, in which the TGBA phase is the only mesophase and the smectic A phase is induced by an electric field. The article is structured as follows. Section 2 presents the observed textures of the TGBA filaments in the studied compound. In sections 3 and 4 the geometry of the TGBA filament is described and the energy of the filament is estimated based on the smectic A elasticity. Together with the observed values of filament dimensions this energy permits discussion of the layer compressibility and estimation of the layer compression modulus B . Finally, the filament model is used in section 5 to explain the observed orientation of the filament.

2. Texture studies

The TGBA textures are studied in different types of the glass cells. Herein, the effect of filaments nucleation is presented for a commercial cell, 5 μm thick, provided with transparent ITO electrodes and with planar anchoring ensured by rubbing a surfactant, with easy direction along the electrode edge. Samples are filled with a new liquid crystalline compound denoted PHB(S) [13] having the enantiotropic TGBA phase in the temperature range from 27°C to 33 °C. A typical texture in a planar sample observed in crossed polarizers on the sample cooled down from the isotropic phase is shown in Fig. 1. This texture contains colored grains, the color corresponding to the pitch length of the TGB helix with the helical axis perpendicular to the sample plane. The spectrometric measurements show the pitch length changing from 380 nm (blue color) to 750 nm (red color) on decreasing temperature within the interval from 32.9 °C to 31.8 °C; for lower temperature the pitch length is out of spectral range. An electric field changes this texture to a homogeneously dark state, showing a uniaxial structure with the optical axis perpendicular to the sample surface. This structure corresponds to a well aligned homeotropic smectic A phase. After the field is switched off a filament texture gradually appears (Figures 2a-c). In Figure 2 the edge of the photographs corresponds to the edge of the electrode, being parallel to the orientation of the crossed polarizers. From these figures one can see that the axes of filaments make a certain angle between 45 and 50 deg with the easy direction at the sample surface (electrode edge). It can be concluded that under the field the director becomes oriented perpendicularly to the sample surface (dark state) and then slowly relaxes to a structure enforced by the planar surface anchoring. The filaments thus originate from the homeotropic state

established by the field. Let us point out that the filament texture is typical for samples with the homeotropic anchoring or the free standing films [5-12].

Based on the dielectric spectroscopy measurements [13], the permittivity, ϵ , has been established in a broad frequency range. We have found that at lower frequencies ϵ_{\parallel} is higher than the permittivity measured on the sample without field application, where the component along the short molecular axis ϵ_{\perp} prevails. Positive dielectric anisotropy, $\epsilon_{\parallel} > \epsilon_{\perp}$, is the reason for the preference of homeotropic alignment under the applied electric field. Thus the transformation of the TGBA phase in the sample with the planar anchoring can be understood as an analogy of the Frederiks transition in nematics [13].

3. Filament of the TGBA phase composed of finite smectic blocks

Rotation of blocks forming the TGBA phase, namely the fact they are finite in all dimensions, is basically responsible for the formation of TGB filaments. The blocks with the structure of the smectic A phase rotate along the axis parallel to the smectic layers, the next blocks being relatively rotated by an angle $\omega = 2\pi l_B / P$, where P is the helical pitch and l_B is the dimension of the blocks along the rotation axis. Then the ratio $P/l_B = N$ is the number of blocks over the pitch length, P . To calculate the free energy of the TGBA phase let us choose the coordinate system connected with unperturbed smectic A layers with the z -axis oriented along the layer normal, and x and y axes in the plane of the smectic layers. The chiral term responsible for layer rotation was proposed in [14] as $-D_2 \frac{\partial \Omega}{\partial x}$ with D_2 as a chiral constant, where $\Omega(x)$

describes the rotation of the blocks around the x -axis at the position x/l_B with respect to the system of unperturbed parallel smectic A layers. This chiral term can be associated with the

elastic curvature term of the type $\frac{K}{2} \left(\frac{\partial \Omega}{\partial x} \right)^2$ where K is the curvature elastic constant of the smectic A, which is isotropic in the xy -plane. Then the curvature part of the free energy density

together with the chiral term can be rewritten as $\frac{K}{2} \left(\frac{\partial \Omega}{\partial x} - q_o \right)^2$ with $q_o = \frac{D_2}{K}$, q_o being

connected with the pitch P as $q_o = \frac{2\pi}{P} = \frac{\omega}{l_B}$. The chirality of liquid crystal, i.e. the sign of q_o , determines the sign of ω .

In infinite blocks the smectic layers are not deformed. Then the minimum of the free energy density leads to the equation $\frac{\partial \Omega}{\partial x} = q_o$ giving continuous rotation of the smectic layers in

the form $\Omega(x) = -\frac{\omega}{2} + \frac{\omega}{l_B} x$. However, the TGB structure consists of discrete rotation of blocks, therefore the form $\Omega(x)$ can be used for geometrical description of TGB phase only when

$x = kl_B$, $k \in (0, N)$ being an integer and N describes the number of blocks within the pitch length, i.e. $N = P/l_B$. The angle $\Omega(x)$ is connected with the density of screw dislocations in TGB walls between blocks.

Above we have outlined a well-known geometrical description of the TGB phase [14 - 16]. In the following, we will describe a nucleation of the TGB phase in the smectic A liquid crystal with the smectic layers parallel to the sample surfaces. Such a situation has been observed in the experiment described in section 2, when the TGBA phase arises from the smectic A phase induced by the electric field (see Fig. 2). In that case the TGBA phase appears in a form of needles (filaments) which are finite in all three dimensions. In the nucleation of filaments both effects of chirality and the surface anchoring preferring the planar molecular orientation are combined.

A nucleus of a block of TGBA phase emerged inside the smectic A phase at the sample surface is schematically shown in Fig. 3. The smectic layers in the block are inclined by an angle Ω with respect to the layers in the surrounding smectic A phase. We suppose that layers in a block are straight except for the sample surface, where they are warped creating a surface *wall of the flexion* there [17] with the edge dislocations accommodating the layer curvature near the surface. The layers parallel to the surface terminate near the inclined block by another system of edge dislocations separated by the distance $b/\tan\Omega$ along the y -axis, b being the layer spacing. In fact the system of edge dislocations forms a boundary, which can be called an *incoherent twin wall* [18, 19] in analogy with twins in solid crystals. For blocks finite along the x -axis the inclination of layers is accommodated by a *twist grain boundary* formed by screw dislocations perpendicular to layers in the block and connecting the edge dislocations with the sample surface (dot-and-dash lines in Fig. 3). Blocks are thus surrounded by parts of dislocation loops starting and ending on the sample surface. The number of the dislocation loops surrounding the block is simply h/b or it can be related to the angle $\Omega(x)$ by the ratio $l/(b/\tan\Omega)$ [18 - 20], h and l being the block height and width, respectively (Fig. 3). On the surface the blocks are ended by a border line (Fig. 3). The border line also terminates the edge dislocation wall on the sample surface. Note that on the other side, at the distance l from the border line (Fig. 3), the block is connected to the system of parallel smectic layers continuously, just by tilt deformation. Such tilt deformation wall is analogous to the *coherent twin wall* [18, 19] in solid crystals. Thus the opposite sides of blocks differ from each other.

The chirality induces a creation of blocks near the surface, where the layers are relatively rotated by an angle ω . Possible situations are shown in Figs. 4 a, b, c. Fig. 4a shows a case when the neighboring blocks are inclined with respect to the unperturbed layers parallel to the sample surface by angles $-\omega/2$ (dashed lines) and $\omega/2$ (full lines), respectively (this situation arises near $x \approx 0$ or $x \approx P/2$). Each block is surrounded by a system of dislocation loops. For simplicity the dislocations are not shown in the figure. Near the sample surface the layers are curved due to the planar surface anchoring. Fig. 4b shows two neighboring slabs with $\omega/2 < \Omega < (\pi-\omega)/2$ i.e. for $0 < x < P/4$. Due to the relative rotation of smectic layers the relative heights of slabs, h_f and h_b could be different. The relative rotation of smectic layers in neighboring slabs

can be seen as relative turning of dashed and full lines where the blocks overlap. Due to this effect the border lines of neighboring blocks are displaced by u . The sign of displacement u is determined by the chirality of liquid crystal, i.e. by the sign of angle ω , which can be seen in Fig. 4b. Rotating of neighboring blocks in Fig. 4b is right-handed. The relative displacement u of the border line (i.e. displacement of layers depicted by dashed lines from layers represented by full lines on the surface) is oriented in the left direction. By changing rotation to left-handed the relative displacement u of border line is oriented to the right. Fig. 4c represents the neighboring blocks inclined with respect to the layers parallel to the sample surface by angles $\Omega = -\frac{\omega}{2} + \frac{\pi}{2}$

(full lines) and $\Omega = \frac{\omega}{2} + \frac{\pi}{2}$ (dashed lines), respectively. Such a situation occurs near $x \approx P/4$.

Simplified 3D view of the filament structure of the length $P/2$ is depicted in Fig. 5, where we envisaged only the smectic layers enveloping blocks terminating on the sample surface (ends of smectic layers of the width l_B form a border line). This view represents the situation when border lines of blocks, depicted as enveloping smectic layers connected to smectic layers parallel to the surface, are relatively shifted by a displacement u on the surface. The shift is due to the block rotation. The more accurate structure of layers is shown in Fig. 4 a-c. Fig. 4a represents the cross-section of the filament layer structure at the front side of Fig. 5. Fig. 4c corresponds to the situation in the center of Fig. 5, where neighboring blocks are continuously reconnected with smectic layers in opposite directions. Fig. 4b shows the situation between the front side and the center of Fig. 5. Smectic molecules in inclined layers are also inclined from the normal of the sample surface. Because of this effect the filament shows an optical contrast in the polarized light with respect to its surroundings.

4. Energy of TGBA filament

In this section we propose an approximate energy of the TGBA filament over the period P . It will enable us to estimate the filament dimensions in directions perpendicular to the rotation axis x , namely the height of k -th block in the z -direction, h_k , and its width, along the y -direction, l_k . Generally, the elastic energies of both screw and edge dislocation walls surrounding each block contribute to the full energy. As for the screw dislocation in the smectic A, recently more detailed solution for a screw dislocation was proposed and a non-zero elastic self-energy was determined [20]. In the limit of an infinite medium, the elastic self-energy given in [21] leads to the Kléman's term $\frac{Bb^4}{128\pi^3 r_o^2}$ [22], where B is the layer compression modulus [14] and r_o is the dislocation core radius. The elastic energy of an edge dislocation per unit length can be written as [17]:

$$E_e = \frac{Kb^2}{2\lambda r_o}, \quad (1)$$

where $\lambda = \sqrt{K/B}$ with the curvature elastic constant K . When comparing (1) with the Kléman's contribution to the screw dislocation energy, it can be found that it is of the order 10^{-3} smaller compared with the energy of an edge dislocation and thus can be neglected and only the elastic energy of an edge dislocation walls will be considered.

The length of the edge dislocations in a wall equals to the thickness l_b of a block along the x -direction is n_k . From Fig. 3 it can be seen that the number of dislocations in the edge dislocation wall is $n_k = l_k / d_k$ and the distance between the edge dislocations along the y -direction is $d_k = b / \tan \Omega(k)$ with $\Omega(k) = -(\omega/2) + \omega k$. Then the edge dislocation wall energy can be approximated as:

$$\sum_{k=1}^N l_b E_e n_k. \quad (2)$$

The chirality leads to a decrease of the energy (per unit volume) $-Kq_o^2$ against to the parallel unwound layers. The energy of the chiral term over the period P is

$$-Kq_o^2 \sum_{k=1}^N l_k h_k l_b, \quad (3)$$

where $l_k h_k l_b$ characterizes a block volume.

The filament is nucleated in the vicinity of the sample surface, where the easy direction affects. Being the axis of the chiral rotation of molecules (i.e. the rotation of layers in the smectic A) along the x -axis, the orientation of the easy direction on the sample surface will be along y -axis. The anchoring energy W_A lowers the total energy by

$$-W_A \sum_{k=1}^N l_k l_b. \quad (4)$$

Then the total energy U of the filament is the sum of expressions (2) – (4). In our model the energy U is taken in an isotropic smectic A liquid crystal. It does not take into account the energy of the layer curvature near the sample surface as we suppose the principal curvature energy is concentrated into edge dislocation walls.

The nucleation of the filament is supported by thermal activation and the driving force is the influence of both chiral term and surface anchoring. The probability of the nucleation is proportional to $e^{-U/kT}$, where k is the Boltzmann constant and T the absolute temperature. The dimensions of a filament h_k and l_k differ with the position of the block along the x -axis. In our simplified model we will use mean values \bar{h} and \bar{l} defined as:

$\bar{h} = \frac{1}{N} \sum_{k=1}^N h_k$, $\bar{l} = \frac{1}{N} \sum_{k=1}^N l_k$ and $\bar{S} = \frac{1}{N} \sum_{k=1}^N l_k h_k$. Area \bar{S} , the mean value of the filament cross-section, can be expressed as $\bar{h}\bar{l}/2$, as it can be seen from Fig 3. Therefore, we take

$$\sum_{k=1}^N l_k h_k l_b \approx N l_b \frac{\bar{h}\bar{l}}{2},$$

and then

$$U \approx l_b E_e \sum_{k=1}^N \frac{h_k}{d_k} - K q_o^2 N \frac{\bar{h} \bar{l}}{2} l_b - W_A N \bar{l} l_b. \quad (5)$$

In the first term of (5) we take the shortest distance between edge dislocations as $d_k \approx b$, which gives the maximum estimation of the edge dislocation wall energy. Taking further $r_o \sim b/2$ [16] and with $N = P/l_B$ we finally obtain

$$U \approx \frac{KP}{\lambda} \bar{h} - K \frac{2\pi^2}{P} \bar{h} \bar{l} - W_A P \bar{l}. \quad (6)$$

Moreover, we can suppose that the mean values of the height and the width of the filament are the same, $\bar{h} \sim \bar{l}$.

The creation of the filament nucleus asks for thermally assisted overcoming of the energy barrier

$\Delta U \approx \frac{KP^3}{8\pi^2 \lambda^2} \left(1 - \frac{W_A \lambda}{K}\right)^2$. This energy barrier is obtained for the critical width of the filament

nucleus \bar{h}_{cr} coming from equation $dU/d\bar{h} = 0$ as:

$$\bar{h}_{cr} = \frac{P^2}{4\pi^2} \left(\frac{1}{\lambda} - \frac{W_A}{K} \right). \quad (7)$$

When the barrier ΔU is overcome, the parameter \bar{h} has the tendency to increase, $\bar{h} > \bar{h}_{cr}$, and the energy U decreases. Further decrease of U can be also obtained when the nucleus elongates in the direction of the filament axis by a length being multiple of the pitch P . Experimental observations show that the elongation of the filament nucleus is much easier along its axis. Our model does not explain this observation but we propose intuitively the following explication. The increase of block dimension needs the further creation of dislocation loops probably near the surface. Edge segments of the created dislocation loop are generally repulsed from the surface [23] but they should move through the whole block. Edge dislocation segment moving through the filament block is then hindered in its motion by so called Peierls-Nabarro barrier (see e.g. [24]) when crossing smectic layers. (The overcoming the Peierls-Nabarro barrier for dislocations in smectic A by the application of an electric field is discussed in [25]). Moreover, for thin samples the other sample surface also repulses edge dislocations thus preventing block growth. Therefore, the filament growth in the direction perpendicular to its axis is hindered with respect to the growth along its axis.

Nevertheless, here we do not treat the dynamics of the filament growth, so our comments on filament propagation are just qualitative. Equation (7) gives the relation between filament parameters, ratio of the elastic constants λ and anchoring energy W_A in our model. From Fig. 2 one can take $\bar{l} \sim \bar{h} \sim 1 \mu\text{m}$. The pitch P can be estimated as $P \sim 0.5 \mu\text{m}$ from the color changes of the texture in Fig.1. With $b \sim 3.6 \text{ nm}$ (see [13]) and a typical value $K \sim 10^{-11} \text{ J/m}$ [14] we obtain a relation between λ and W_A . We have found the electric field starts to change the planar texture to a homogeneously dark state at about 10 V. The completely homogeneous dark state is, however,

reached at about 50 V when the electric field expels the most of defects. The voltage 10 V at the beginning of transformation of planar texture to homogeneous one enables us to estimate the value of the anchoring energy of molecules at the sample surfaces. The energy of the electric field E in the volume of the sample thickness t and unit sample surface is $-\frac{\varepsilon_o \varepsilon_a}{2} E^2 t$ where ε_a is a dielectric anisotropy and ε_o is the vacuum dielectric constant, $\varepsilon_o = 8.854 \times 10^{-12}$ F/m. The experiment shows $\varepsilon_a \sim 1$, see Ref. [13]. The thickness of the studied sample is about 5 μm . Comparison of anchoring energy $2W_A$ (per unit surface) on both sample surfaces with the energy $\frac{\varepsilon_o \varepsilon_a}{2} E^2 t$ gives the estimation of the anchoring energy:

$$W_A \approx \frac{\varepsilon_o \varepsilon_a}{4} E^2 t. \quad (8)$$

From relation (8) we obtain $W_A \sim 4.2 \times 10^{-5}$ J/m². This anchoring energy is comparable with the typical values of anchoring energies of nematic liquid crystal spanning from 10^{-5} to 10^{-7} J/m² [26]. Then equation (7) gives $\lambda \sim 6.2 \times 10^{-9}$ m and $B \sim 2.6 \times 10^5$ J/m³. Note, however, that the estimation of λ for a typical smectics in [14] is about $\lambda \sim b \sim 3 \times 10^{-9}$ m, which corresponds to $B \sim 10^6$ J/m³. It means that the studied smectic material PHB(S) is relatively soft, i.e. exhibits higher compressibility, which is consistent with other experimental data. The length of the extended molecule of PHB(S) has been calculated to be 3.1 nm, which is less than the measured layer spacing, which is about 3.6 nm [13]. It can be explained by a mutual lengthwise shift of molecules within the smectic layers, which results in higher degree of layer compression in the studied compound.

5. Orientation of the filament axis

Textures described in section 2 show that the filaments are usually inclined from the easy direction of the anchoring at the sample surface. We want to demonstrate that this inclination is connected with the widths of blocks, l_b , and their relative displacements u along the y -axis (see Figs. 4b, 5). The position of the k -th block along the x -axis can be written as $x_k \approx l_b k$ but we approximate limits of blocks by continuous lines in the xy -plane. Let the characteristic length L of blocks in filament be $L = \sqrt{h^2 + l^2}$ (see Fig. 3). Then we can determine the projection of the filament on the sample surface by limits y_1 and y_2 of a block along the y -axis which depend on the coordinate x . In this model we neglect the layer curvature nears the surface shown in Fig. 3.

Using this concept of block rotation with constant L , limits y_1 and y_2 can be expressed for $x \in (0, P/4)$ as $y_1 = \frac{u}{l_b} x$ and $y_2 = \frac{u}{l_b} x + L \cos \Omega(x)$.

For $x \in (P/4, P/2)$ we have $y_1 = \frac{u}{l_b} x - L \left(\cos \Omega(x) + \sin \left(\frac{\omega}{2} \right) \right)$ and $y_2 = \frac{u}{l_b} x - L \sin \left(\frac{\omega}{2} \right)$,

for $x \in (P/2, 3P/4)$ we have $y_1 = \frac{u}{l_b}x - L\left(\cos\left(\frac{\omega}{2}\right) - \sin\left(\frac{\omega}{2}\right)\right)$ and

$$y_2 = \frac{u}{l_b}x + L\left(\cos\Omega(x) + \cos\left(\frac{\omega}{2}\right) - \sin\left(\frac{\omega}{2}\right)\right).$$

Finally, for $x \in (3P/4, P)$ it is $y_1 = \frac{u}{l_b}x - L\left(\cos\Omega(x) - \cos\left(\frac{\omega}{2}\right)\right)$ and $y_2 = \frac{u}{l_b}x + L\cos\left(\frac{\omega}{2}\right)$.

Continuity of y_1 and y_2 at points $x \rightarrow P/4, P/2, 3P/4$ is assured. The filament axis can be described as the mean value of the filament limits y_1 and y_2 , i.e. $y = (y_1 + y_2)/2$. In Fig. 6 the projection of filament blocks on the sample plane xy is schematically drawn together with the filament axis, the orientation of which changes along x -axis. In our model the filament width also changes along the axis of block rotation as it is proportional to the projection of L into the plane of the sample surface.

In the following we determine the mean angle of filament axis inclination from the easy direction of the planar surface anchoring. The tangent of the filament axis y for $x \in (0, P/4)$ and $x \in (P/2, 3P/4)$ is

$$\frac{dy}{dx} = \frac{u}{l_b} - \frac{L}{2} \frac{\omega}{l_b} \sin\Omega(x), \quad (9)$$

while for $x \in (P/4, P/2)$ and $x \in (3P/4, P)$ it is $\frac{dy}{dx} = \frac{u}{l_b} + \frac{L}{2} \frac{\omega}{l_b} \sin\Omega(x)$.

Then the mean value of the tangent $\langle dy/dx \rangle = \langle \tan\alpha \rangle$ over the period P gives

$\langle \tan\alpha \rangle = \frac{1}{P} \int_0^P \frac{dy}{dx} dx = \frac{u}{l_b}$. Therefore the inclination angle α of the filament axis with respect to

the x -axis is principally given by the ratio u/l_b . The inclination from the easy direction is

$\frac{\pi}{2} - \alpha$. (see Fig. 6). As the sign of displacement u is determined by the sign of chirality, the

angle α has the same property. This is the reason why we observe just one orientation of the filament axis with respect to the easy direction.

The displacement u can be expressed as multiple of the layer spacing value b . The observations show that the inclination of the filament axis with respect to the easy direction is about 45-50 deg., which gives the displacement $u \approx l_b$. Taking the estimation of the block width $l_b \approx 18$ nm [16], we obtain $u \approx 5b$. In the present model of the filament description the displacement u is constant, which describes in the simplest way the observed filament axis inclination with respect to the easy direction of the surface anchoring. In this way the displacement u is connected with the angle of relative block rotation ω which is also constant. The local rotation axis between neighboring blocks is parallel to the x -axis but its position in z -direction can differ from block to block.

6. Discussion

The presented simplified model of TGB filaments is based on the nucleation of the TGB phase on the surface, the liquid crystal chirality and the surface anchoring being effective. Due to a relative rotation of neighbor blocks their ends at the surface are shifted by a displacement u . This explains why the mean filament axis is inclined with respect to the easy axis of the surface anchoring. Let us point out that such inclination has been observed previously [6], but has remained unexplained.

Filaments can be created also in the sample bulk. In such a case the filament blocks of TGB phase behave very similarly to bulk twins in solids. The layers in a block are continuously connected to surrounding smectic layers along two opposite faces (coherent twin walls). The other four side faces are enclosed with closed dislocation loops having the edge and screw components as it is schematically depicted in [15]. The screw components are situated between neighboring blocks (twist grain boundaries), while the edge components discontinuously connect surrounding smectic layers (incoherent twin walls). Naturally, the creation of a bulk filament is not assisted by the surface anchoring.

Observations show also filaments in the direction nearly perpendicular to the direction of the majority of the surface filaments (see Fig. 2a). We expect that these filaments are nucleated on already grown primary filaments and are probably directed obliquely to the bulk. Due to repulsion of the edge dislocations surrounding the primary and bulk filaments the interaction energy in the mutually perpendicular directions is minimized.

The anchoring energy can be estimated from the critical value of the electric field starting the transition of the TGBA phase to the homeotropic order with layers parallel to the glass plates. From the experiments this value has been established to be about 10 V. This value corresponds to the anchoring energy about $4.2 \times 10^{-5} \text{ J/m}^2$, which is comparable with typical anchoring energies of nematics on rubbed glass [26]. From equation (7) the compressibility modulus can be determined as $B \sim 2.6 \times 10^5 \text{ J/m}^3$. This value is lower compared to the classical smectic A phase modulus $B \sim 10^6 \text{ J/m}^3$, showing relatively higher compressibility of the studied liquid crystal in the smectic A phase. This fact is in accordance with the results obtained from the smectic layer thickness measurements showing that the layer thickness is higher than the length of an extended molecule. Both facts can be explained by a concept of layers composed of molecules associated in pairs, the cores being relatively shifted with respect to each other. Layers with mutually shifted molecules can be compressed more easily than in smectics with the layer thickness comparable to the molecular length.

7. Conclusions

We present a model of filaments based on the observations of the chiral liquid crystal PHB(S) exhibiting the isotropic-TGBA phase sequence without any intermediate cholesteric or blue phases. Under an applied electric field the TGBA phase is transformed to the smectic A phase with the homeotropic structure, which is homogeneously dark in crossed polarizers, showing thus quite perfect alignment. The model describes gradual arising of the TGBA phase in the form of filaments from the field induced homeotropic smectic A phase after the field is

switched off. This process starting at the sample surface is driven by chiral forces in combination with the planar anchoring. Finite blocks of TGBA structure, which compose a filament, are separated from neighboring filament blocks by dislocation loops having screw and edge components and starting and finishing on the sample surface. Screw components of the dislocation loops form twist grain boundaries between blocks in a filament. Edge components of the dislocation loop form incoherent grain boundary between a block and homeotropic smectic A layers on one side of the block while the other side is continuously connected to surrounding homeotropic smectic A layers (coherent grain boundary) as seen in Fig. 3.

From the value of the surface anchoring, W_A , estimated from the experiment, relatively high compressibility of the studied liquid crystalline compound can be deduced. The model of the filament is also able to explain the observed orientation of the filaments with respect to the easy direction of the anchoring on the sample surface. It is worth pointing out that the creation of similar filaments is typically observed in other compounds during the smectic A-TGBA phase transition under a temperature change and up to now has not been theoretically described and explained.

Acknowledgements

This work was supported by the Czech Science Foundation (project 15-02843S).

References

- [1] W. T. Read: *Dislocations in Crystals* (McGraw Hill Publ. Co., New York, 1953).
- [2] P. G. de Gennes, *Solid State Commun.* **10**, 753 (1972).
- [3] Renn, S.R.; Lubenski, T.C. *Phys. Rev. A* **38**, 2132 (1988).
- [4] J. W. Goodby, M. A. Waugh, S. M. Stein, E. Chin, R. Pindak, and J.S. Patel, *J. Am. Chem. Soc.* **111**, 8119 (1989).
- [5] N. Podoliak, V. Novotná, M. Kašpar, V. Hamplová, M. Glogarová, and D. Pociеча, *Liq. Cryst.* **1**, 176 (2014).
- [6] I. Dierking, *Textures of Liquid Crystals*, (WILEY-VCH, Weinheim, 2003).
- [7] I. Dierking, and S.T. Lagerwall, *Liq. Cryst.* **26**, 83 (1999).
- [8] J. W. Goodby, S. J. Cowling, and V. Görtz, *C.R. Chimie* **12**, 70 (2009).
- [9] M. Kašpar, V. Novotná, V. Hamplová, M. Glogarová, and D. Pociеча, *Liq. Cryst.* **37**, 129 (2010).
- [10] V. Novotná, M. Glogarová, V. Kozmík, J. Svoboda, V. Hamplová, M. Kašpar, and D. Pociеча, *Soft Matter.* **9**, 647 (2013).
- [11] H.-S. Kitzerow, and C. Bahr, *Chirality in Liquid Crystals*, (Springer-Verlag, New York, 2001).
- [12] R. Dhar, *Phase Transitions* **79**, 175 (2006).
- [13] J. Novotná, M. Glogarová, M. Kašpar, V. Hamplová, L. Lejček, and D. Pociеча, to be published in *Soft Matter*.

- [14] P. G. de Gennes, and J. Prost: *The Physics of Liquid Crystals*, 2nd ed. (Oxford University Press, Oxford, 1993).
- [15] M. Kléman, and O. D. Lavrentovich: *Soft Matter Physics: An Introduction* (Springer – Verlag, New York, 2003).
- [16] P. Oswald, and P. Pieranski: *Smectic and Columnar Liquid Crystals* (Taylor and Francis, Boca Raton, 2006).
- [17] M. Kléman, *Points, Lines and Walls in Liquid Crystals, Magnetic Systems and Various Ordered Media* (J. Wiley , New York, 1983).
- [18] M. Brunet, L. Lejček, and L. Navailes, *Ferroelectrics* **244**, 323 (2000).
- [19] M. Brunet, L. Lejček, L. Navailes, P. Keller, H. T. Nguyen, E. Polossat, and E. Rouy, *Liq. Cryst.* **33**, 981 (2006).
- [20] L. Lejček, *Czech. J. Phys.* **40**, 1250 (1990).
- [21] Fan Tian-You, and Li Xian-Fang, *Chin. Phys. B* **23**, 046102 (2014).
- [22] M. Kléman, *Phil. Mag.* **34**, 79 (1976).
- [23] L. Lejček, and P. Oswald, *J. Phys. II France* **1**, 931 (1991).
- [24] L. Lejček, *Czech. J. Phys. B* **32**, 767 (1982).
- [25] R. Holyst, and P. Oswald, *J. Phys. II France* **5**, 1525 (1995).
- [26] A. A. Sonin, *The Surface Physics of Liquid Crystals* (Gordon and Breach Publishers, Luxembourg, 1995).

Figure Captions:

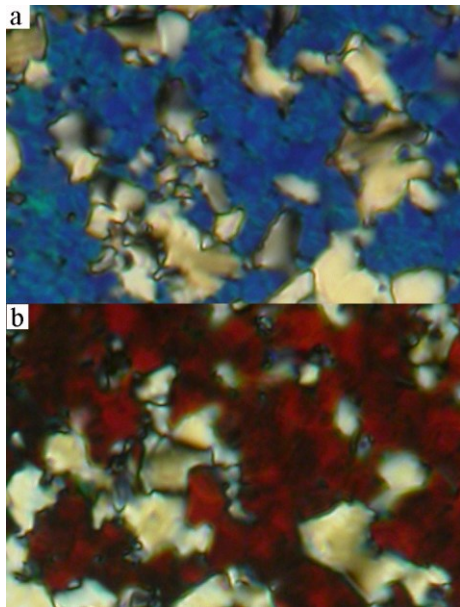


Figure 1: Nucleation of the TGBA phase in PHB(S) compound when cooling down the sample. (a) TGBA phase exhibits blue color at the temperature 33°C, (b) the color of TGBA phase changes to red one at the temperature 32.2°C. The width of every micrograph is about 120 μm .

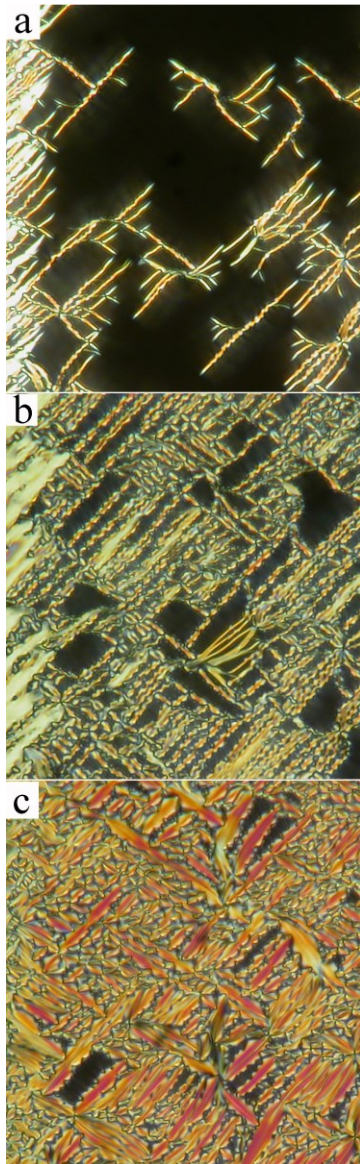


Figure 2: The growth of filaments of the TGBA phase in the homeotropic state of PHB(S) compound after switching off the electric field, temperature 32.2°C.

(a) Individual filaments grow with time in the direction making an angle between 45 and 50 deg. with the easy direction at the sample surface. The easy direction is parallel to the edge of electrode parallel with the edge of the Figure. (b) The density of filaments increases with time, sometimes also filaments perpendicular to the primary system of filaments occur. (c) When filaments cover all the sample, an individual filament can coalesce making wider areas of TGBA phase. The width of every micrograph is about 150 μm .

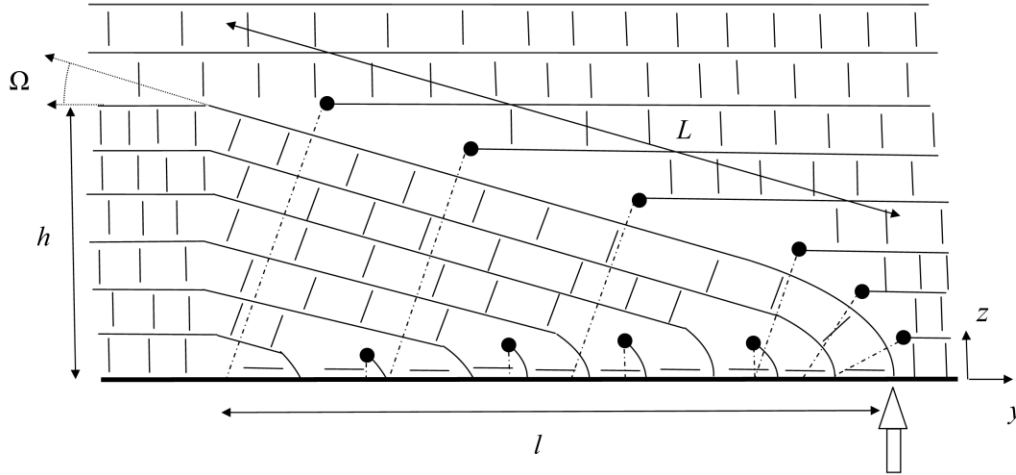
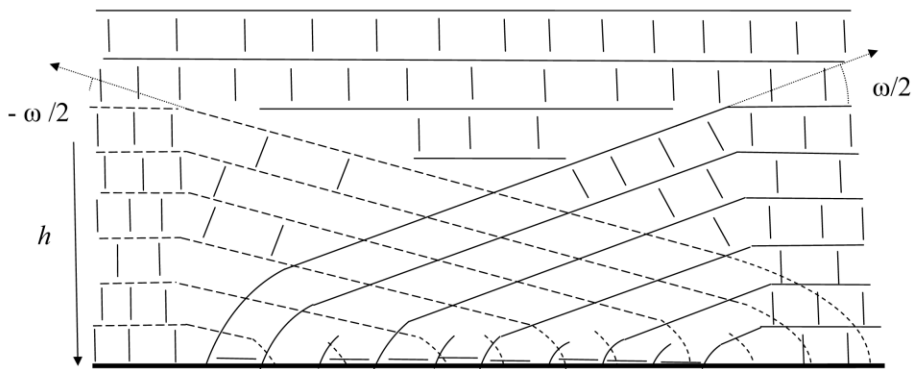


Figure 3: Schematic representation of a block with the smectic A layers inclined by an angle Ω with respect to layers parallel to the sample surface (thick line). The smectic layers are represented by thin lines with molecules shown as short line segments. The full dots show cross-sections of edge dislocations, which are connected with the sample surface by a system of screw dislocations (dot-and-dash lines). The open arrow shows the position of a border line of the inclined block at the surface, the line being parallel to the x -axis. Dimensions of block are the height h and width l determining the characteristic length L as $L = \sqrt{h^2 + l^2}$. The y and z -axes are indicated, the x -axis is perpendicular to the plane of figure.

(a)



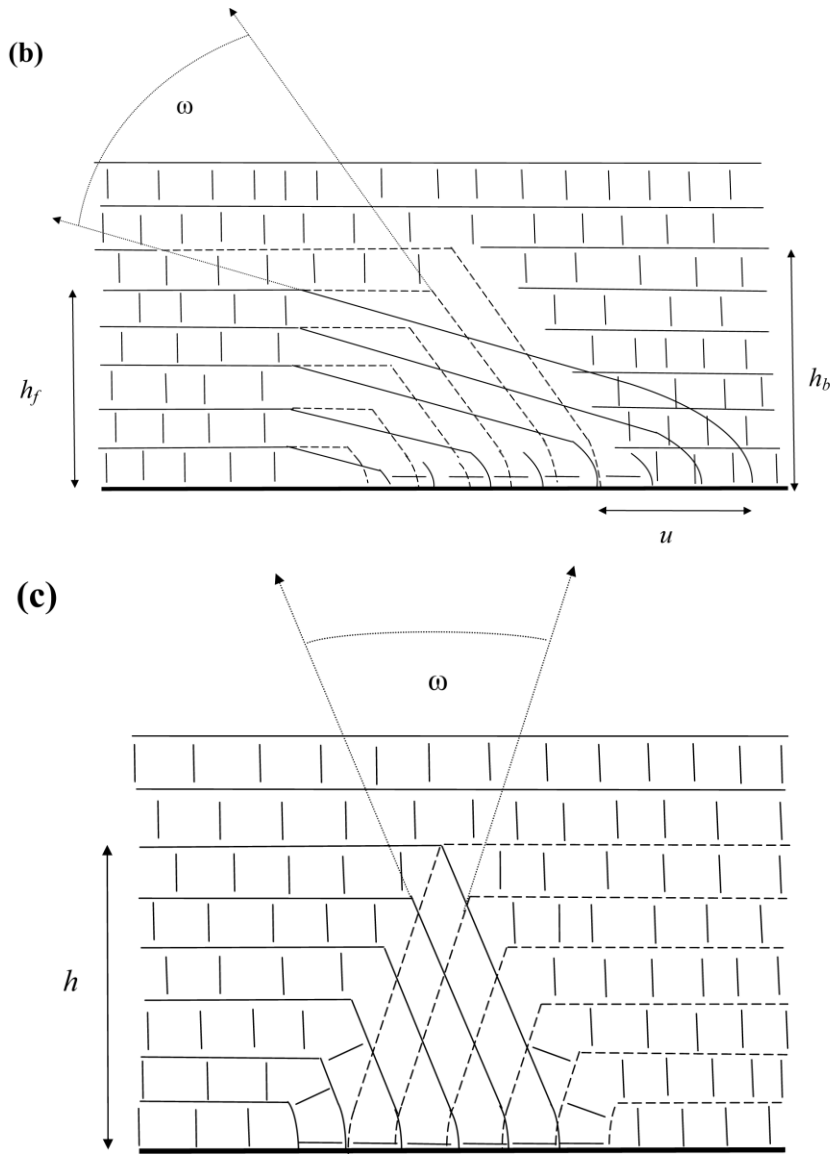


Figure 4: Schematic representation of two neighboring blocks shown in full and dashed lines (a) blocks at $x \sim 0$ and $x \sim P/2$ inclined by an angle $\frac{\omega}{2}$ and $-\frac{\omega}{2}$ with respect to the parallel smectic layers and thus mutually inclined by ω . The height, h , of both blocks is equal. (b) an example of two neighboring blocks in the interval $0 < x < P/4$, the heights of both blocks are different h_f and h_b . Displacement u is a shift of the border lines of these blocks. (c) two neighboring blocks near $x \approx P/4$ mutually inclined by ω .

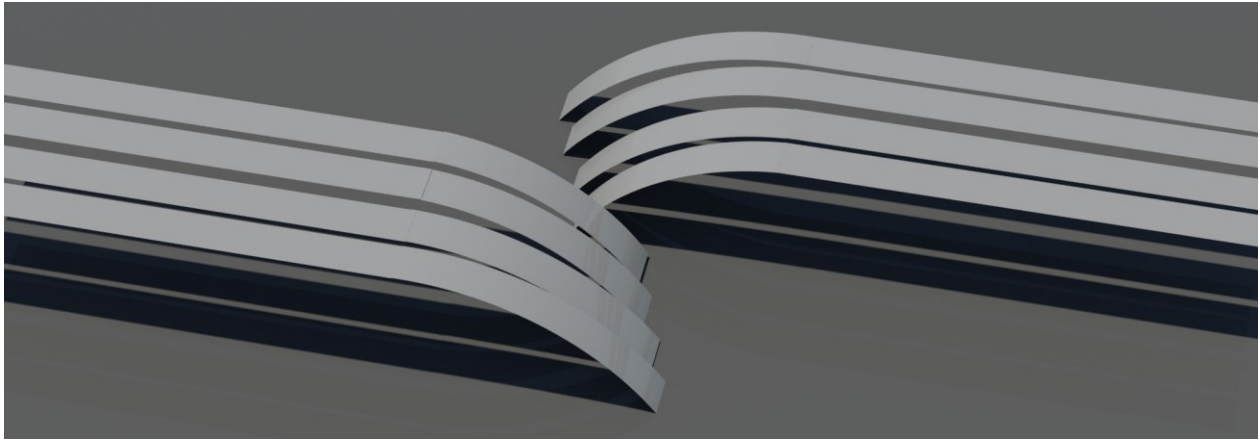


Figure 5: 3D drawing of the smectic layers which terminate on the sample surface tracing there a border line. Depicted smectic layers constitute an envelope of the filament only. The presented simplified view demonstrates namely a relative displacement of neighboring blocks on the sample surface caused by chirality induced relative block rotation. The filament segment presented has the length of $P/2$.

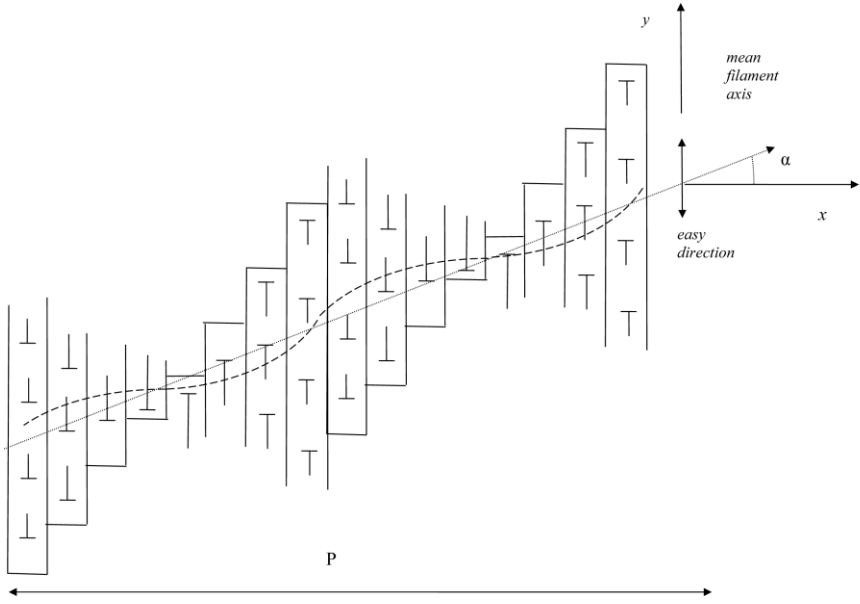


Figure 6: Schematic drawing the filament seen along the normal to the sample surface. Block rotations lead to the inclination of molecules from the sample surface normal, along which the sample is observed. Inclined molecules are represented by nails the points of which are oriented toward the observer. The length of the nails corresponds to the projection of the inclined molecule to the sample plane. Relative block rotations are illustrated by nails of different lengths in neighboring blocks. The helix axis is parallel to x -axis. Along the helix axis the molecules rotate by 2π . The direction of the filament axis (dashed line) depends generally on the position along the filament. The mean filament axis (dotted line) is inclined with respect to x -axis by an inclination angle α . The easy direction of the surface anchoring is parallel to y -axis.